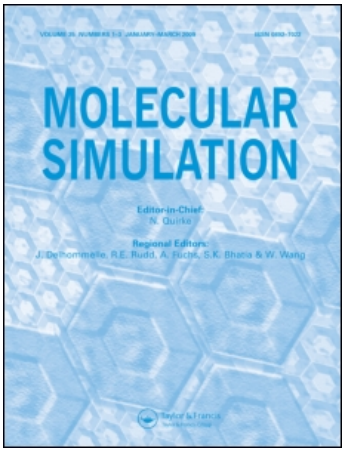

Molecular Simulation
Publication details, including instructions for authors and subscription information:
http://www.informaworld.com/smpp/title~content=t713644482

Monte Carlo Simulations of the Chemical Potential and Free Energy for Trimer and Hexamer Rings

R. E. Randelman[ab]; Gary S. Grest[a]; M. Radosz[a]
[a] Corporate Research, Science Laboratory, Exxon Research and Engineering Company, Annandale, New Jersey, USA [b] Department of Chemical Engineering, Lehigh University, Bethlehem, Pennsylvania, USA

To cite this Article Randelman, R. E. , Grest, Gary S. and Radosz, M.(1989) 'Monte Carlo Simulations of the Chemical Potential and Free Energy for Trimer and Hexamer Rings', Molecular Simulation, 2: 1, 69 — 88
To link to this Article: DOI: 10.1080/08927028908032784
URL: http://dx.doi.org/10.1080/08927028908032784

Molecular Simulation, 1989, Vol. 2, pp. 69–88
Reprints available directly from the publisher
Photocopying permitted by license only

MONTE CARLO SIMULATIONS OF THE CHEMICAL POTENTIAL AND FREE ENERGY FOR TRIMER AND HEXAMER RINGS

R.E. RANDELMAN†, GARY S. GREST and M. RADOSZ

Corporate Research, Science Laboratory, Exxon Research and Engineering Company, Annandale, New Jersey 08801 USA

(*Received September 1987; in final form February 1988*)

The chemical potential of a trimer and hexamer model ring system was determined by computer simulation over a range of temperatures and densities. Such ring molecules are important as model aromatic and naphthenic hydrocarbons. Thermodynamic integration of the pressure along a reversible path, Widom's ghost particle insertion method and Kirkwood's charging parameter method were used over a molecular density range of 0.05 to 0.30. Data were obtained by Monte Carlo simulation of a 96 molecule system that was modelled with a Lennard-Jones 6–12 truncated potential. The original insertion method, which does not take into account the orientation of the molecule when it is inserted, gives results for the chemical potential which deviate from that obtained using the thermodynamic pressure integration. At high density or temperature the deviation is significant. We have modified the Widom insertion technique to account for this short range orientation and find good agreement between this technique and the thermodynamic integration method for the chemical potential. We also calculated the free energy difference between our model ring molecules and ring molecules made up of hard spheres.

KEY WORDS: Chemical potential, ring systems, Monte Carlo simulation

1 INTRODUCTION

In the liquid phase, the chemical potential, along with the free energy, are two of the most important and elusive quantities to determine in any thermodynamic study. They are needed to quantify phase equilibria which, in turn, form the basis for separation processes. Only recently have techniques been proposed to calculate these parameters using molecular dynamics (MD) and Monte Carlo (MC) simulations. To our knowledge, most of these studies have concentrated on determining the chemical potential and free energy for simple fluids made up of spherical particles or mixtures of two spherical particles [1–10]. In addition, there have been a few studies for systems consisting of diatomic molecules and mixtures [11,12]. Since most fluids of industrial and technological interest are neither spherical nor dumbbell in shape, it is important to determine if the computer simulation methods presently available to obtain the free energy and chemical potential are also applicable to systems consisting of more complex molecules. One particular concern is that as the complexity of the molecule increases the ghost particle insertion methods, now widely used to determine the chemical potential, may only be applicable at too low a density to be useful. This is

†Also at Department of Chemical Engineering, Lehigh University, Bethlehem, Pennsylvania 18015 USA.

because at higher densities the chance of an overlap insertion increases and as the molecules get larger, the overlap condition may occur for lower densities.

For these reasons we have initiated a study to determine the chemical potentials and Helmholtz free energy for a pure fluid made up of ring molecule. Such molecules are important as simple models of aromatic and naphthenic hydrocarbons. We applied three methods: the standard thermodynamic integration of the pressure along a reversible path, Widom's ghost particle insertion method and Kirkwood's charging parameter method to calculate the chemical potential, μ. We find that the original insertion methods, which do not take into account the orientation of the inserted molecule, are not applicable for complex molecules. Instead, one must modify the manner in which the molecules are inserted to account for the fact that all orientations of the inserted molecule are not equivalent. We have developed a procedure using a Boltzmann weighting over many random orientations of the inserted molecule to account for this orientational effect. We call this insertion technique the modified Widom method and find excellent agreement with the thermodynamic integration of pressure method for μ.

For free energy, we used the overlap method and thermodynamic integration. The purpose was to test the regime of density and temperature that these methods may be applicable for complex molecules. Since in previous work only one of these methods is usually applied to a particular model, it is important to carry out careful comparisons of the applicability of these methods for a wide range of density and temperature.

In the next two sections we describe the methods and equations used to determine the chemical potential and free energy from computer simulations. In Section 4, we present our results and in Section 5 we summarize and present our conclusions. In the Appendix, we give details of the model system and the Monte Carlo simulation technique.

2 CHEMICAL POTENTIAL

The standard technique for determining the free energy or chemical potential using computer simulation is to carry out a thermodynamic integration along a reversible path. While in principle any set of thermodynamic variables could be used, one method could be to integrate the pressure as a function of density. We call this technique pressure integration. The chemical potential μ^r can be obtained from

$$\mu^r = \frac{A^r}{N} + \frac{P}{\varrho} - kT \tag{1a}$$

where A^r is the residual Helmoltz free energy, T is temperature, k is Boltzmann's constant, N is the number of molecules, V is the volume, $\varrho = N/V$ is the number density, and A^r is the residual Helmoltz free energy,

$$\frac{A^r}{N} = kT \int_0^{\varrho} \frac{1}{\varrho'} \left[\frac{P}{\varrho' kT} - 1 \right] d\varrho'. \tag{1b}$$

For the pure ideal gas $\mu^r = A^r$. The pressure, P, can be obtained from the virial theorem:

$$PV = NkT - \frac{1}{3} \sum_{i>j}^{N} r_{ij} \frac{d}{dr_{ij}} \Phi(r_{ij}) \tag{1c}$$

where $\Phi(r_{ij})$ is the interaction potential energy function between molecules i and j.

While the pressure integration method is straightforward, in practice there are two difficulties. First, many intermediate states are necessary to evaluate Equation (1a) accurately, most of which are at low densities and hence uninteresting. Second, to obtain data using Monte Carlo simulations for the pressure near a phase transition, it may be necessary to impose extra constraints on the system in the coexistence region. Hansen and Verlet [13], in their study of the phase diagram of atomic Lennard-Jones systems, created van der Waals loops in the liquid-gas coexistence region by limiting the allowed density fluctuations in the system. This technique has been widely used for it created a reversible path along which Equation (1b) could be integrated and until recently was the only method available for obtaining chemical potentials or free energies numerically. However, other techniques have been developed which are generally more efficient and accurate than pressure integration.

A more direct method which can be used to determine the chemical potential, called the ghost particle insertion method, has been developed by Widom [14], Bennett [15] and others, and reviewed by Quirke [5] and Heinbuch and Fischer [6]. Powles *et al.* [7] have demonstrated that the advantage of this method is that the chemical potential can be calculated from the ratio of two distribution functions, $G(u)$ and $F(u)$, which themselves can be determined numerically at relatively small additional computational expense. Here $G(u)$ is the distribution function for the potential energy of the Nth molecule in an N-molecule system and $F(u)$ is the fictitious or ghost particle distribution function. The function $F(u)$ describes the distribution of the potential energy required to insert the $(N + 1)$th molecule randomly into an N-particle system without dislocating the other N molecules. Once these two distribution functions are determined, the chemical potential can be easily obtained.

The chemical potential is defined as

$$\mu = \frac{\partial A}{\partial N}|_{V,T} = \lim_{n\to\infty} [A(N, V, T) - A(N\text{-}1, V, T)] \tag{2a}$$

where A is the Helmholtz free energy

$$A = -kT\ln Q \quad \text{where} \quad Q = \int \exp(-\beta U(\mathrm{q}_i^{\mathrm{N}})\, dq^{\mathrm{N}}). \tag{2b}$$

In terms of the difference in Helmholtz free energy for two systems 0 and 1 one can write [7]

$$\begin{aligned} Q_0/Q_1 &= \exp\{-\beta(A_0 - A_1)\} \\ &= \int \exp(-\beta U_0) dq^{\mathrm{N}} / \int \exp(-\beta U_1) dq^{N} \\ &= \langle \exp(-\beta(U_0 - U_1))\rangle_1. \end{aligned} \tag{3a}$$

Here $\beta = 1/kt$ and $\langle \ldots \rangle$ is a canonical average over system 1. Alternatively,

$$Q_0/Q_1 = 1/\langle \exp(-\beta(U_0 - U_1))\rangle_0 \tag{3b}$$

A normalized distribution function for any coordiante-dependent quantity x, can be defined as: $f_i(x) = \langle \delta(x(q) - x)\rangle$, where $\delta(z)$ is the Dirac delta function. Powles *et al.* [7] have shown that when U_0-U_1 equals u, equations (2a, 2b) can be expressed as

$$f_0(u) = \exp(-\beta u) f_1(u) \langle Q_1/Q_0\rangle. \tag{4}$$

If we let system 0 have N particles and system 1 have N-1, then U_0-$U_1 = u(N; N\text{-}1)$

is the energy of the Nth particle in the N-particle system. This would correspond to a system in which an additional fictitious particle is inserted into the N-1 particle system. Then Equation (3a) can be written as [7]

$$Q_0/Q_1 = \langle \exp(-\beta u_f) \rangle_{N-1}, \tag{5a}$$

where $u_f \equiv u(N; N\text{-}1)$, since the Nth particle does not interact with the other (N-1) particles. Then from Equations (2b) and (3b) we find

$$Q_0/Q_1 = \exp(-\beta\mu^r) = \langle \exp(-\beta u_f) \rangle_{N-1}. \tag{5b}$$

Here μ^r is the residual chemical potential, μ-μ^{id}, and μ^{id} is the chemical potential of an ideal gas with $U = 0$. μ^{id} can be represented as $T \ln \varrho$-$3/2 T \ln T$, (neglecting the quantum mechanical energy term: $3/2 T \ln [h^2/2\pi m\varepsilon\sigma^6]$), so that $\mu \simeq \mu_1 = \mu^r + T \ln \varrho - 3/2\ T \ln T$.

Equations (3–5) can be rearanged in a convenient form for computing μ^r [7],

$$L(u) \equiv \ln [F(u)/G(u)] = \beta u - \beta\mu^r. \tag{6}$$

Here $F(u) \equiv f_0(u)$ and $G(u) \equiv f_1(u)$ and a plot of $L(u)$ vs. u gives a slope of β and intercept at $u = 0$ of $-\beta\mu^r$.

Shing and Gubbins [8] and De Oliviera [16] have shown that the chemical potential can also be obtained based on Equation (3b)

$$\exp(\beta\mu^r) = \langle \exp(\beta u_r) \rangle_N. \tag{7}$$

Here $u_r = u(N; N\text{-}1)$, following Powles *et al.* [7], since this is the interaction energy for the real Nth particle in the N-particle system. Clearly from Equations (5b) and (7)

$$\langle \exp(-\beta u_f) \rangle_{N-1} \langle \exp(+\beta u_r) \rangle_N = 1, \tag{8}$$

which can be a test of the consistency while calculating the chemical potential.

For simple monotonic fluids, it is clear how to calculate the ghost particle distribution, $F(u)$. One simply inserts the molecule at a large number of random positions in the sample and measures the energy distribution. However, it is not clear how $F(u)$ should be determined for complex molecules which are not necessarily spherical. Obviously, one must choose the center of mass at random, but there is clearly an ambiguity in determinating the molecular orientation. The derivation above suggests that one should also choose the orientation of the molecule at random. This is in fact what has been done in earlier calculations for dumbbell molecules [1,3,4]. However, as we will show in Sect. 4, this is in general not correct. One way to see why this procedure cannot be correct is to remember that to determine μ from Eq. (6), one is interested in the ratio $F(u)/G(u)$. Here $G(u)$ is the distribution of potential energies for the molecules in equilibrium. If the molecules are not isotropic, then there will be a short range order which effects the packing of the molecules and therefore $G(u)$. Consequently, to obtain the correct result for μ, the determination of $F(u)$ should account for the fact that the energy to insert a molecule is indeed orientation dependent.

We have employed a modified insertion technique to determine $F(u)$ which accounts for this orientational dependency in the insertion of the fictitious molecule. Rather than use one trial set of Euler angles for each random choice of the center of mass selected, a number of random Euler angle sets are chosen and a Boltzmann average of the resultant energies used to determine the potential, u. The Boltzmann

average is defined as:

$$u = \frac{\sum_{M} U \exp(-U/kT)}{\sum_{M} \exp(-U/kT)} \tag{9}$$

where U is the energy of the inserted molecule and M is the number of random selections of the Euler angle set (θ, ϕ, ψ). We call this distribution of modified insertion energies, $F^*(u)$. The resultant chemical potential determined from the ratio $F^*(u)/G(u)$ is much lower than when the orientation of the molecule is neglected. We found that in most circumstances there was little difference in using the minimum energy or the Boltzmann average. Obviously M must be large to determine the insertion energy, u, accurately. In the present simulations, we find that it was sufficient to use $M = 100$, but clearly as the complexity of the molecules increases, so must M.

In our numerical studies, we used all three of the above formulations to determine μ^r. We found, as did Powles *et al.* [7], that the graphical method utilizing Equation (6) was generally more reliable than Equations (5b) and (7). These equations would require knowledge of the distributions over the entire range of energies u, and hence are less reliable. We also found that averaging over the fictitious distribution $F^*(u)$ generally gave the same result from Equation (5b) as the graphical determination of μ^r. However, when averaged over $G(u)$, we find that Equation (7) usually gave incorrect results for μ^r. This is because the regions where $G(u)$ is small and therefore not determined very accurately give large contributions to the average.

The ghost particle insertion methods are limited to moderate densities because, as the density increases, the percentage of useful insertions decreases rapidly. For example, for the hexamer model at a density of $\varrho\sigma^3 = 0.15$, the percentage of insertions in which the inserted molecule does not overlap the other molecules is approximately 3%. By contrast, the percentage of non-overlapping insertions at $\varrho\sigma^3 = 0.05$ is approximately 40%.

A complimentary insertion method can be used at higher densities to obtain the chemical potential. In this method, the chemical potential is the sum of two contributions. The first is obtained from insertion of a smaller molecule into the system using a technique similar to the Widom method. The second is obtained by a thermodynamic integration of the potential energy over several intermediate systems which have N-1 normal molecules and one smaller one [17].

In simulation, the system is then described as the N-1 normal size molecules with bond length γ, along with the one particle with bond length $\zeta\gamma$. Here ζ is the fractional size of the test particle to the others and is called the charging parameter. Shing and Chung [18] have derived the Kirkwood chemical potential equation for solutions and an equivalent form for pure components can be represented as

$$\mu^r = kT \ln \left| \frac{N \Lambda^3}{\langle V \rangle q} \right| + \int_0^1 \langle \Delta\Phi \rangle_\zeta d\zeta \tag{10}$$

where $\langle \Delta\Phi \rangle_\zeta \equiv \Phi_1 - \Phi_2$. Φ_1 is the energy of the smaller molecule in the system and Φ_2 is the energy if the smaller molecule were a molecule with $\zeta_i = 1.0$. Such a system with one smaller molecule of size ζ_i is termed to have a coupling parameter of ζ. $\langle V \rangle$ is the NPT ensemble average volume, Λ is the thermal deBroglie wavelength and q is the molecular partition function. Shing and Chung [18] have shown that one could also write this as

$$\mu^r = -\mu^{id} + \int_0^1 \langle \Delta\Phi \rangle_\zeta d\zeta \tag{11}$$

However, in the case where can obtain the chemical potential for a certain system with coupling parameter ζ_i by the modified Widom's method, where the ghost particle inserted has bond length $\zeta_i\gamma$, we can write

$$\mu^r = \mu^r_{\zeta_i} + \int_{\zeta_i}^1 \langle \Delta\Phi \rangle_\zeta d\zeta. \tag{12}$$

Thus the chemical potential for both moderate and high densities can be obtained using $\mu^r_{\zeta_i}$ with a combination of the modified Widom method along with an energy integration from ζ_i to 1.

The test particle inserted has fractional size ζ_i, and ζ_i is determined as the largest value for the test particle that gives good statistical data. Whenever possible we choose $\zeta_i = 1$, in which the Kirkwood method and the previously described Widom methods yield equivalent results, except that the Kirkwood method is done at constant pressure whereas the Widom methods are done at constant volume.

When $\zeta_i < 1$, then a separate series of simulations are done to evaluate the average at enough points so that the integral in Equation (12) can be evaluated numerically. In practice, five to ten points are obtained for the integrand.

3 FREE ENERGY

The residual Helmholtz free energy, defined as $A^r/NkT = (A\text{-}A^{id})/NkT$, can also be obtained from computer simulations by several methods [5]. One method is the thermodynamic integration technique based on Equation (1b). With this method, A^r/NkT is calculated directly, but has similar disadvantages as the pressure integration method discussed above for the chemical potential. An alternative method is the overlap ratio method which follows from the fact that the free energy difference between two systems can be written as

$$\frac{A_1}{NkT} - \frac{A_0}{NkT} = -\ln \frac{Q_0}{Q_1}. \tag{13}$$

Here Q is defined by Equation (2b) and A_1 and A_0 are the free energies of two systems. 0 and 1. It can be shown [5] that $\Delta A = A_1 - A_0$ can be written as

$$\exp \Delta\left(\frac{A}{kT}\right) = \frac{f_0(\Phi)}{f_1(\Phi)} e^{\Phi}. \tag{14a}$$

Here

$$f_0(\Phi') = \frac{1}{Q_0} \int \exp(-U_0/kT)\, \delta((U_0 - U_1)/kT - \Phi')\, d^N q \tag{14b}$$

and $f_1(\Phi')$ is a similar distribution averaged over system 1.

The two distribution functions in Equation (14a) and their overlaps are evaluated to yield the free energy difference. When the potentials are very dissimilar, such as Lennard-Jones and hard core, the overlap in the distributions could be very small or non-existent. This leads to a situation in which intermediate states are used to bridge the two systems of interest [19a].

Although a choice of the reference system A_0 is arbitrary, its free energy has to be known. A particularly good choice is a system that can be described by an exact equation of state, because the free energy could be determined analytically for any state point. However, for simple model fluids which contain more than two interaction centers, no equation of state is sufficiently accurate. Therefore to test the available methods, we measured the free energy of a system of ring molecules that interact only via a hard core repulsion as a reference. This is similar to earlier studies for atomic [19a] and dumbbell systems [19b].

Specifically, our reference system is composed of ring molecules with hard core spheres. Our focus is on the free energy difference between a ring of particles interacting with a Lennard-Jones potential Φ and an identical ring interacting with hard core potential, $H(\sigma_h)$. If we let U_0 be the Lennard-Jones potential, Φ, and U_1 be the Lennard-Jones potential plus a hard core potential, $\Phi + H(\sigma_h)$, with atomic diameter, σ_h, then Equation (14a) becomes [19a]

$$\Delta A = -\ln(\langle \exp(-H/kT)\rangle_0) \equiv -\ln g. \tag{15}$$

The Boltzmann factor, $\exp(-H/kT)$, is either zero or one for all configurations with potential U_0 depending on whether any site-site distance $r_{a\beta}$ is less than or greater than σ_h. The average in Equation (15) is the fraction of the configurations for which all $r_{a\beta} > \sigma_h$. This is called the virtual overlap method since only configurations with no overlaps are counted. This last equation can be used to calculate $\Delta(A/kT)$ as long as σ_h is not too small thereby giving no overlaps and $g = 1$.

If the reference system of interest has a hard core diameter σ_h so large that $g = 0$, one can still use Equation (12) since it is also true if $U_0 = \Phi + H(\sigma_{h1})$ and $U_1 = \Phi + H(\sigma_{h2})$, where $\sigma_{h2} > \sigma_{h1}$. The virtual overlap method can then be used with a finite number of intermediate configurations using a stepwise progression from the value of σ_h where $g > 0$ to the σ_h of interest. Once the free energy between Lennard-Jones and Lennard-Jones plus a fixed hard core is obtained, the overlap ratio method by Equation (14), is used to determine the second part of the free energy between $\Phi + H(\sigma_h)$ and $H(\sigma_h)$. the two parts can then be combined to obtain the free energy difference between rings interacting with the Lennard-Jones and hard core potentials.

To relate this free energy difference to the residual free energy obtained by the pressure integration, the free energy difference between the hard core and an ideal reference state is needed. We have tried to use the results of Nezbeda [19] for oblate spherocylinders, to obtain the free energy of the hard core system, by relating the geometries of our hard-core ring molecules to oblate spherocylinders, using both a geometric and volumetric similarity.

4 RESULTS

4.1 Chemical Potential

The pressure integration method requires pressure isotherms, such as those shown in Figure 1, for the trimer at three temperatures, $T = 2$, 4 and 6, where we can define a reduced density, ϱ^* as $\varrho^* = \varrho\sigma^3$. The isotherm $T = 2$ in this figure is clearly below the critical point and $T = 4$ and 6 are above. As can be seen, in the range $0.01 < \varrho^* < 0.08$ the isotherm has a nearly zero slope for $T = 2$ but not for the other two temperatures. The very small, nearly constant, values for the pressure make

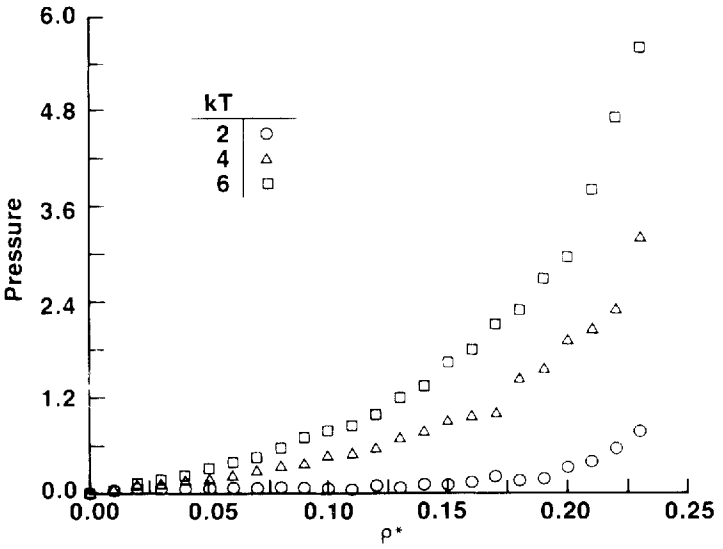

Figure 1 Trimer pressure as a function of density, ϱ^*, for $T = 2, 4, 6$ from simulation data using Equation (1c). $T = 2$ is below the critical point.

the integration at $T = 2$ difficult since small fluctuations in the pressure tend to give erroneous fluctuations in the integral. The slopes for $T = 4$ and 6 in the low density region are larger and hence one expects that more confident values for the integral can

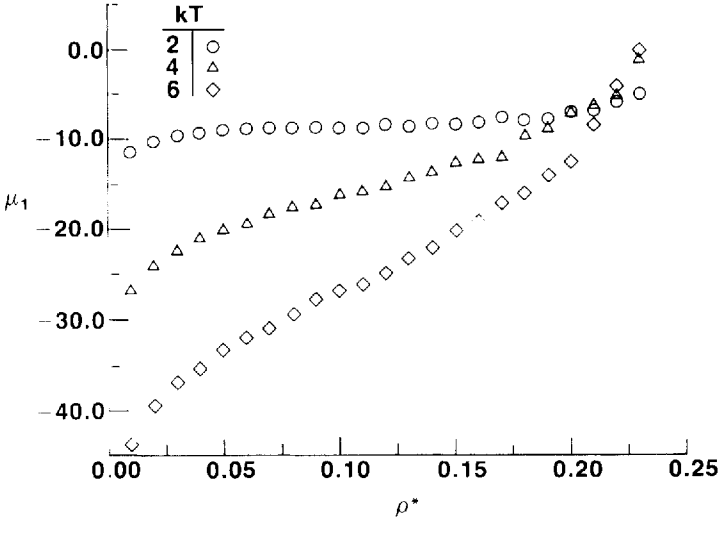

Figure 2 μ_1 for trimer system from integration of the pressure data using Equation (1b, 1c) and correcting for temperature and density effects as described in the text.

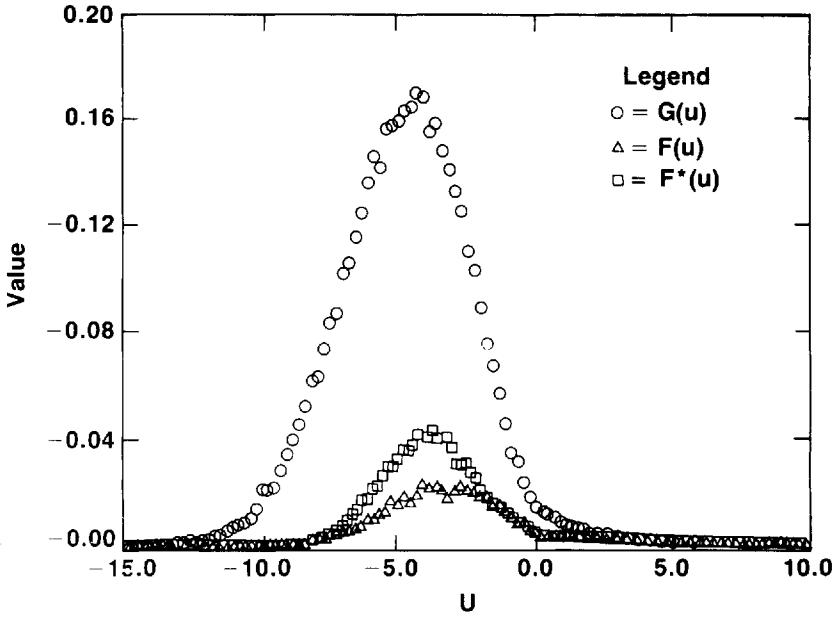

Figure 3 Distribution functions $G(u)$, $F^*(u)$ and $F(u)$ for the ghost particle insertion method with trimers at the $T = 4$, $\varrho^* = 0.10$ space point.

be obtained. Figure 2 shows the chemical potential, μ_1, obtained from the pressure integration. The curves show decreasing μ_1 for increasing temperature. An inversion hump is seen for $T = 2$, while the curves monotonically increase for $T = 4$ and 6.

In addition to the pressure integration, Widom's method was applied for a number of state points (T, ϱ^*). Figure 3 shows the distribution functions $G(u)$, $F(u)$ and $F^*(u)$ for ($T = 4$, $\varrho^* = 0.10$). As can be seen there is a difference in the overlaps between $G(u)$ and $F(u)$, and $G(u)$ and $F^*(u)$. At this point, both sets of distributions show very good overlap, with the modified insertion overlap maximum occurring near $u = -4.0$.

Figures 4a and 4b show the results for $\ln[F(u)/G(u)]$ and $\ln[F^*(u)/G(u)]$ for various densities at $T = 4$. Note that from these data alone there is no indication which combination gives the correct values of the chemical potential. Both ratios, $F(u)/G(U)$ and $F^*(u)/G(u)$, give reasonable results for the chemical potential. All the curves in Fig. 4 have the correct slope of $1/kT$; however, the intercepts are quite different, resulting in different values for μ^r. As the density increases, the $u = 0$ intercept decreases but the slope remains nearly constant. The scatter at large positive values of u is due in part to large positive energy changes with small changes in the intermolecular distance as two trimers approach each other. In addition, for these state points, it is expected that statistically few of the trimer pairs would yield positive potential energies. The scatter at higher densities is due to an increase in the frequency of ghost particle insertions which overlap with other molecules and corresponding reduction in good statistics. Much longer simulations would, however, correct this. The fraction of negative ghost insertion energies decreases rapidly for increasing density and very much longer simulation would be needed to obtain μ by direct

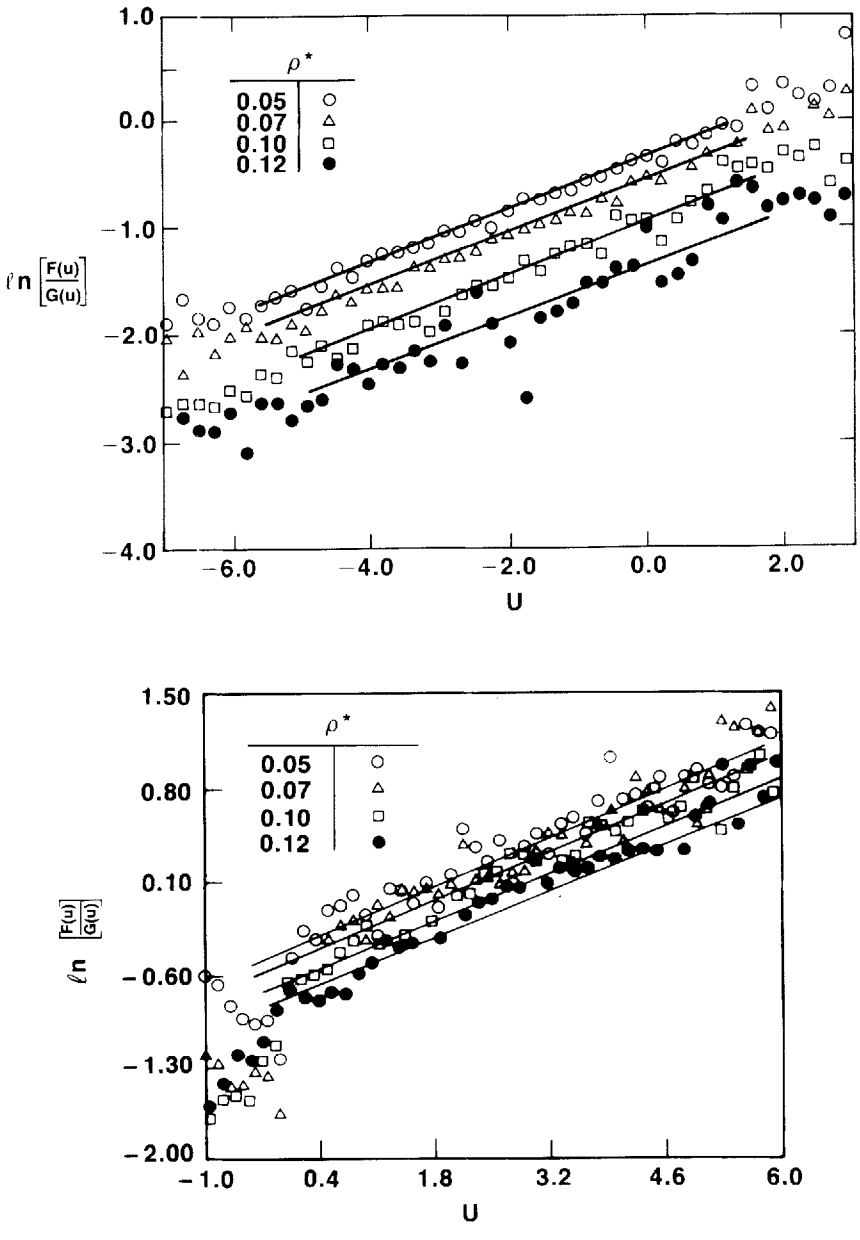

Figure 4 Ghost and real energy distributions for the trimer model for $T = 4$ and various densities plotted in the form of Eq. (6) a) using $F(u)$ and $G(u)$ b) using $F^*(u)$ and $G(u)$. The slope equals β and remains constant for different densities while the intercept at $u = 0$, $-\beta\mu^r$, increases. From the data alone, it is not possible to say which set, a or b, is correct.

insertion for $\varrho^* > 0.16$. Table 1 summarizes our results for the chemical potential for several temperatures and densities using the modified Widom method and pressure integration for the trimer.

Using the unmodified insertion technique, the agreement between the integration and insertion methods, as shown in Figure 5, is reasonable for low densities or sub-critical temperatures, but very poor for higher densities or temperatures. This agreement at low density is due mainly to the small relative contribution of μ^r to μ_1 at low densities and the small differences in $F(u)$ and $F^*(u)$. However, as density increases the two methods give very different results for μ^r, and this difference is clearly seen even in μ_1. It is important to note that this disagreement is in fact the only indication that the unmodified insertion technique is incorrect. Other internal checks of this method give no indication that a break down of the technique had occurred. The slope of the curves plotted in Fig. 4 have the correct temperature, also the summation of the insertion energy distribution, Eq. (8), gave the same result for μ^r as the graphical method.

In contrast, the modified insertion technique gives very good agreement over most of the density range for all temperatures and all the consistancy checks as described above are also satisfied. Only this direct comparison to the pressure integration data shows that the original Widom's method predicts too large a value for μ.

In the hexamer simulation the interactions are stronger and, as a result, obtaining good data from the simulations required more computer time. Three temperatures, $T = 6, 10, 15$, were chosen, corresponding to below the critical point, at or near the critical point, and above the critical point. Figure 6 shows the pressure isotherms for these temperatures. The $T = 6$ pressure isotherm is quite flat in the low density limit, dropping in the middle region and rising modestly at higher densities. Such a curve is characteristic of a liquid below its critical temperature. The curves for $T = 10$ and

Table 1 Results for trimer molecules. Integration refers to the pressure integration method and insertion refers to the modified ghost particle insertion technique. Fraction of insertion acceptance is the fraction of the ghost particle insertions which yield negative energies. Insertion correlation is the X^2 correlation coefficient from the least squares analysis of Equation (6).

kT/ε	$\varrho(\sigma^3)$	*Integration* μ^r	*Integration* μ_1	*Insertion* μ^r	*Insertion* μ_1	*Fraction of Insertion Acceptance*	*Insertion Correlation*
2.0	0.05	−1.10	− 9.17	−2.57	−10.64	0.67	0.96
2.0	0.07	−1.59	− 8.99	−3.28	−10.68	0.55	0.98
2.0	0.10	−2.12	− 8.81	−4.05	−10.78	0.38	0.98
2.0	0.12	−2.34	− 8.66	−4.38	−10.70	0.28	0.98
2.0	0.15	−2.57	− 8.44	−4.56	−10.48	0.16	0.98
4.0	0.05	−0.097	−20.39	−0.768	−21.07	0.65	0.97
4.0	0.07	0.03	−18.92	−0.849	−19.80	0.52	0.97
4.0	0.10	0.34	−17.18	−0.584	−18.11	0.35	0.98
4.0	0.12	1.05	−15.83	−0.131	−16.93	0.25	0.98
4.0	0.15	2.41	−13.48	1.23	−14.68	0.13	0.98
6.0	0.05	0.935	−33.14	0.544	−33.55	0.62	0.95
6.0	0.07	1.65	−30.43	1.08	−31.00	0.50	0.97
6.0	0.10	3.31	−26.62	2.34	−27.60	0.34	0.98
6.0	0.13	4.74	−24.11	3.64	−25.20	0.24	0.98
6.0	0.15	7.17	−20.41	6.46	−21.05	0.13	0.99

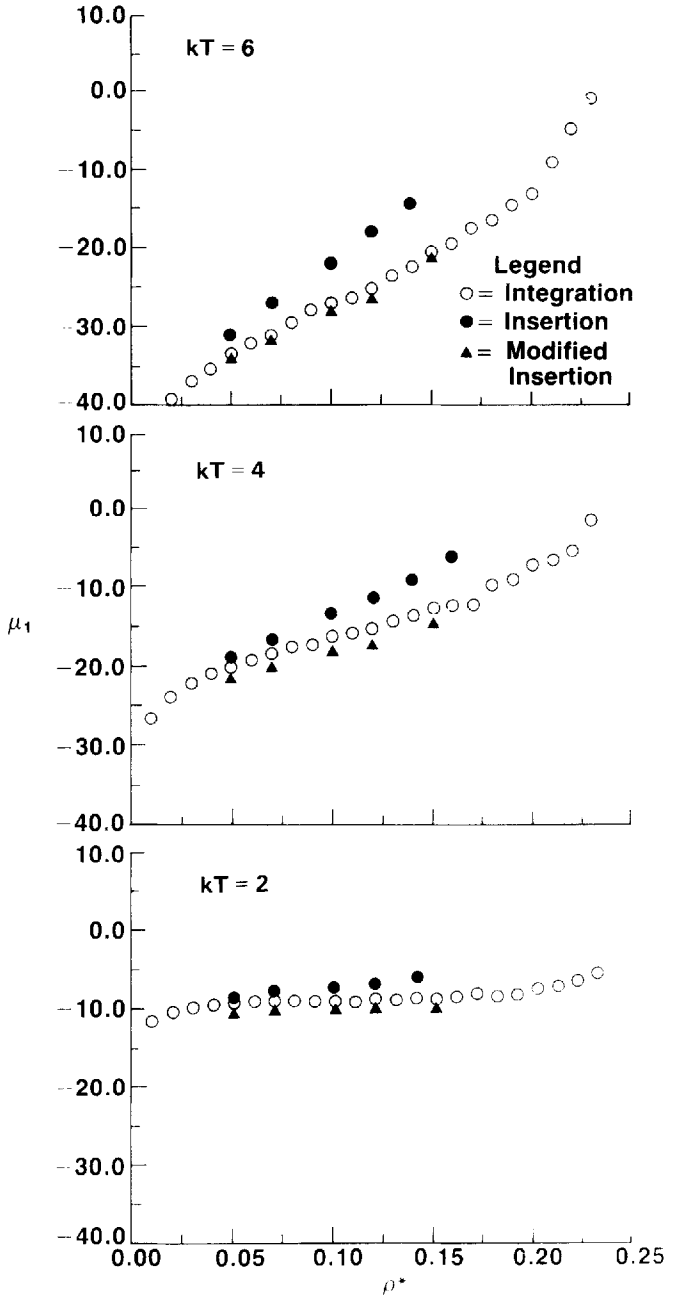

Figure 5 Comparison of μ_1 for ghost particle insertion and pressure integration methods for the trimer system at $T = 2, 4, 6$. Open circles, closed circles and closed diamonds correspond respectively to pressure integration, Widom insertion, and Modified Widom insertion methods. As exhibited, the modified Widom insertion method gives significantly better agreement.

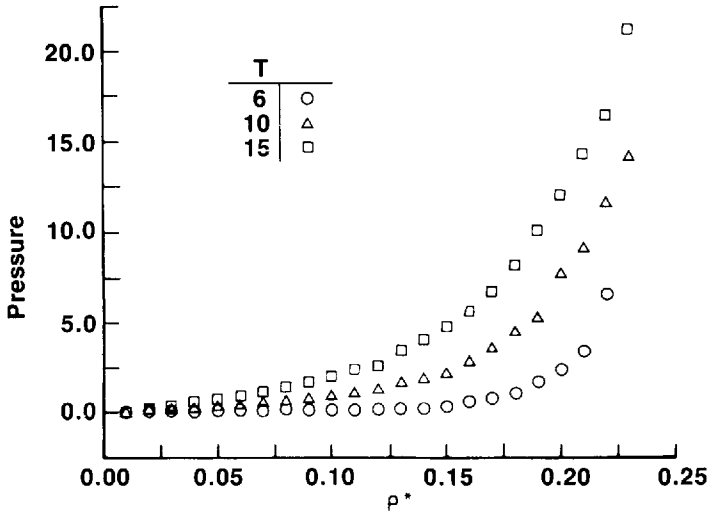

Figure 6 Hexamer pressure as a function of density, ϱ^*, for T = 6, 10, 15 from simulation data using Equation (1c). $T = 6$ is below the critical point.

15 have greater slopes for the high density region and a lower density onset of the breakpoint of the change in slope. In addition, the curve for $T = 15$ has a noticeable and monotonic increase in pressure for all densities.

Figure 7 compares μ_1 for the three methods at $T = 15$, and two methods at $T = 10$ and 6. For the points obtained from the unmodified insertion, the agreement with the pressure integration over the range is merely acceptable at $T = 6$, but at $T = 10$ and 15, the agreement degrades considerably. In contrast, using modified insertion the agreement improves dramatically. Over nearly the entire range of pressure and density there is excellent agreement with the pressure integration. We reiterate, unless a direct comparison to the pressure integration method was made, both insertion techniques would give all indications that they were accurate. It is only by the integration versus insertion comparisons that a significant problem is exhibited in the original insertion method, which is then resolved using the modified approach.

When we applied the Kirkwood method for $\varrho^* > 0.12$, we used the largest value for ζ_i that would yield good insertion statistics. This value was usually either 0.5 or 0.4, except at $\varrho^* = 0.25$ where $\zeta_i = 0.2$. We found that for each density the value for $\Delta\Phi$ was nearly constant over the range of integration, $\zeta_i \to 1.0$. The Kirkwood method was checked at two points whose chemical potential were previously determined using the modified Widom's insertion method. The methods agree within 5%. The deviations in μ_1 between the Kirkwood method and the direct modified insertion with $\zeta_i = 1.0$ are believed to be largely due to the uncertainty in determining $\mu^r_{\zeta_i}$, for $\zeta_i = 1.0$. The Kirkwood method with $\zeta < 1.0$ gives a more accurate determination since the number of acceptances is larger, albeit at the expense of having to make several additional runs using intermediate systems over the range of ζ_i. Table 2 summarizes the simulation results for the hexamer using the modified ghost particle insertion, pressure integration, and Kirkwood methods.

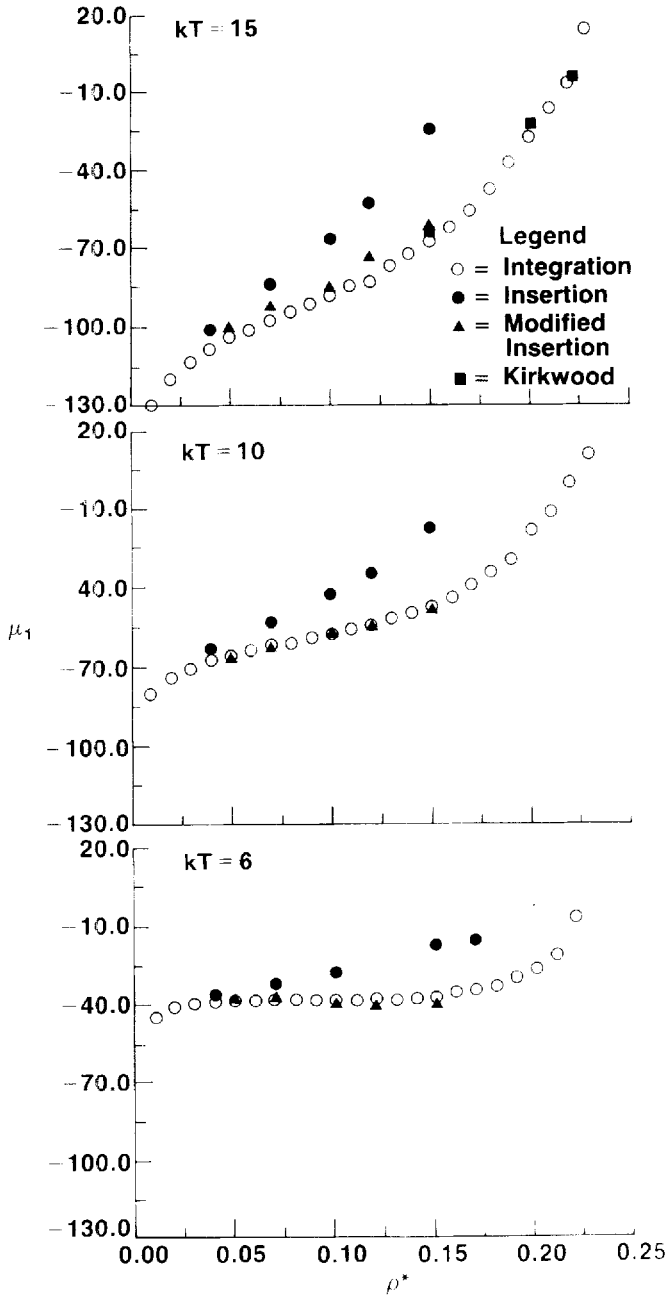

Figure 7 Comparison of μ_1 for the ghost particle insertion, Kirkwood method, and pressure integration methods for the hexamer system at $T = 15, 10, 6$. Open circles, closed circles, closed diamonds and closed squares correspond respectively to pressure integration, Widom insertion, modified Widom insertion, and Kirkwood methods. As in the trimer, the modified Widom insertion method gives significantly better agreement.

Table 2 Results for hexamer molecules. Integration refers to the pressure integration method and insertion refers to the ghost particle insertion technique. Fraction of insertion acceptance is the fraction of the ghost particle insertions which yield attractive potentials. Insertion correlation is the X^2 correlation coefficient from the least squares analysis of Equation (6).

kT/ε	$\varrho\sigma^3$	*Integration* μ^r	*Integration* μ_I	*Insertion* μ^r	*Insertion* μ_I	*Kirkwood* μ^r	*Kirkwood* μ_I	*Fraction of Insertion Acceptance*	*Insertion Correlation*
6.0	0.05	−2.16	−36.71	−2.26	−36.36			0.60	0.97
6.0	0.07	−3.67	−35.76	−3.42	−35.50			0.46	0.98
6.0	0.10	−4.13	−34.07	−7.30	−37.24			0.22	0.97
6.0	0.12	−5.27	−34.12	−8.89	−37.74			0.12	0.98
6.0	0.15	−6.70	−34.20	−9.23	−36.73			0.02	0.97
10.0	0.05	−0.51	−65.00	0.77	−65.27			0.56	0.99
10.0	0.07	−0.09	−61.21	−0.12	−61.26			0.40	0.98
10.0	0.10	1.62	−55.94	1.57	−55.99			0.20	0.98
10.0	0.12	2.96	−52.78	2.03	−53.71			0.10	0.98
10.0	0.15	7.15	−46.36	6.56	−46.94			0.03	0.97
15.0	0.05	0.75	−105.11	4.44	−101.42			0.53	0.97
15.0	0.07	2.21	−98.61	7.45	−93.36			0.39	0.98
15.0	0.10	5.60	−89.86	9.96	−85.50			0.22	0.98
15.0	0.12	10.17	−82.51	18.03	−74.70			0.09	0.97
15.0	0.15	21.31	−68.06	25.56	−63.82	23.91	−65.48	0.03	0.98
15.0	0.20	55.37	−29.69			37.31	−25.76		
15.0	0.22	79.50	−4.17			50.89	−8.83		

4.2 Free Energy

The residual free energy was determined using the pressure integration and overlap ratio methods. The overlap ratio method was used to obtain the trimer free energy, the free energy difference with hard core reference system using $\sigma_h = 0.97\sigma$. Because the potentials were very different, between 7 and 15 intermediate steps were necessary to determine the free energy difference. As expected, the free energy difference of these states increased with increasing density. Increasing the density further beyond $\varrho^* = 0.15$ would require a greater number of intermediate states to determine the free energy accurately.

Table 3 summarizes our results for a trimer system at $T = 4$ and $\sigma_h = 0.97$ for three densities: $\varrho^* = 0.07$, 0.10 and 0.15. The first method obtained the virtual overlap term by multiplying the g from Equation (15) for each of the individual intermediate states. This gives the free energy difference between a Lennard-Jones potential and a Lennard-Jones plus hard core potential. The overlap ratio is obtained by comparing the energy of a Lennard-Jones plus hard core potential obtained during a simulation run under a hard core potential, to the energy of a hard core potential when the simulation is run under Lennard-Jones plus hard core. Such ratios are then used with Equation (14a) to generate the free energy difference between a system with Lennard-Jones plus hard core potential and a pure hard core potential. When these two contributions are multiplied, the result is the free energy difference between a system with a Lennard-Jones potential and a reference system with a pure hard core potential. The last row in Table 3 shows the result from the pressure integration in which the free energy difference is A^r as described in equation (1b).

Table 3 Results for the free energy calculation for the trimer at $T = 4$. Integration refers to the residual free energy from pressure integration. Overlap refers to the hard core reference free energy computed by the virtual overlap methods with a hard core reference of $\sigma_h = 0.97$.

$T = 4.0$ *Trimer*		$\varrho\sigma^3 = 0.07$	$\varrho\sigma^3 = 0.10$	$\varrho\sigma^3 = 0.15$
Virtual Overlap:	# Intermediate States	7	10	15
$\sigma_{hl} = 0.97\sigma$	Q_1/Q_0	1.24×10^{-3}	8.18×10^{-5}	5.47×10^{-6}
Overlap Ratio:				
$\sigma_{hl} = 0.97\sigma$	Q_1'/Q_0'	0.4822	0.7689	1.292
$\ln\left(\frac{Q_1'}{Q_0'} \cdot \frac{Q_1}{Q_0}\right)$	$\frac{A^{HC}}{kT}$	−7.42	−9.67	−16.46
Thermodynamic Integration	$\frac{A^{ID}}{kT}$	4.72	9.69	22.46

We cannot directly compare the overlap and pressure integration methods since their reference states are different and the free energy of the hard core system is not known. We attempted to determine the hard core reference free energy using the Nezbeda [20] model. However, for our system no suitable geometry was found that would yield reliable results since the range of the reference free energy was inconsistent with our simulation data. The overlap method, although applicable to all densities, can only therefore give the free energy differences and not the absolute values, unless the free energy of the reference system is known.

For our particular case of hard core reference, we found that for low to moderate densities the number of intermediate states seem to be of the order of $100\varrho^*$; however, at $\varrho^* > 0.16$, the number of intermediate states increases quickly. We started the method at $\sigma_{hl} = 0.80$ where $g = 1.0$ and increased σ_{hl} as much as possible at each intermediate step until the corresponding g was less than 0.10.

5 CONCLUSION

There appears to be no single approach to obtain the chemical potential for these model trimer and hexamer ring systems. If the interest is in the range of chemical potentials, perhaps the pressure integration technique is best since once the pressure curve is determined, any chemical potential in that density range can be obtained. However, if the chemical potential is required at a few densities, especially high densities or low temperatures, then the modified insertion technique would be preferred.

We believe that the disagreement between the original insertion and integration methods is due mainly to the short range anisotropy of the system. This difference is only weakly shown in μ_1 at low densities where the contribution of μ^r to μ_1 is small and since structuring effects are at a minimum, there is little difference between $F(u)$ and $F^*(u)$. At higher densities, however, μ^r gives a large contribution to μ_1 and, as seen

in Figures 5 and 7, the methods strongly disagree. This disagreement increases with increasing molecular-model complexity.

We have modified the Widom insertion method to account for this short-range ordering effect. This modified insertion and the pressure integration methods gave results for the chemical potential which are in very good agreement. At high densities, the Kirkwood technique was shown to agree well with the pressure integration and the modified Widom insertion method. Since the dominant term in the Kirkwood method is the insertion contribution, this is not surprising.

The pressure integration results can also be used to determine the free energies relative to the ideal gas. The other method used to obtain the free energy, the overlap method, cannot be compared directly because it uses a different reference, the hard core potential. The hard core reference used was found to be too removed from the model fluid to allow deriving absolute values for the free energy.

Further work includes using the insertion techniques to determine the chemical potential of more realsitic ring molecules and mixtures, needed in modeling hydrocarbon separations, and a more complete investigation of the anisotropic effects.

Acknowledgement

The authors would like to thank Katherine Shing, Keith Gubbins, Nicholas Quirke and Doros Theodorou for their many helpful discussions that aided this work.

APPENDIX

Most of the simulations were run on a 96 molecule system consisting of either trimer or hexamer rings. The geometry can be described as an N-gon with the center of each atom located a distance b from the center of mass of a planar molecule. The interaction between atoms was chosen to be a Lennard-Jones (6–12) site-site potential with a cutoff at $r_c = 2.0\sigma$.

$$\Phi(r) = 4\varepsilon\left[\frac{\sigma^{12}}{r^{12}} - \frac{\sigma^6}{r^6} - \frac{\sigma^{12}}{r_c^{12}} + \frac{\sigma^6}{r_c^6}\right] \quad r \leqslant r_c \tag{16}$$

$$\Phi(r) = 0 \quad r > r_c \tag{16}$$

Here we choose $b = \sigma/\sqrt{3}$, which yields a length between adjacent atoms of σ. The trimer simulations were run at temperatures $kT/\varepsilon = 2, 4, 6$ and hexamer at $kT/\varepsilon = 6$, 10, 15. These temperatures were selected to cover the range from below to above the critical point. In the remainder of the paper we set the energy ε and length σ in reduced units to 1, and define a reduced density $\varrho^* = \varrho\sigma^3$.

A standard Metropolis [21] Monte Carlo simulation was performed in which the molecules were placed in a cubic box with length, L, and cyclic boundary conditions. Most of the simulations where run at constant volume except for those used in the Kirkwood method, Equation (12), which were run at constant pressure.

For the constant volume case, the total ensemble energy, E, is calculated. The center of mass of a molecule is then moved by a random amount

$$\vec{r} = [\delta\vec{x}, \delta\vec{y}, \delta\vec{z}] \quad \text{such that} \quad -\Delta \leqslant r \leqslant \Delta.$$

The molecule is then rotated by randomly changing the three Euler angles (θ, ϕ, ψ)

so as to sample phase space uniformly. Two of the Euler angles, ϕ and ψ, take values on the interval $0 \leqslant \phi, \psi \leqslant 2\pi$ and are changed by selecting a new angle from uniform deviates in the range $(0, 2\pi)$. θ is defined over the range $0 \leqslant \theta \leqslant \pi$, such that $\cos(\theta)$ is sampled uniformly in the range $(-1, 1)$ [22].

Once the new center of mass and Euler angles are determined, the energy, E_1, of the new configuration is calculated. If $\Delta E = E_1 - E \leqslant 0$ the move is accepted while if $\Delta E > 0$, the move is accepted with probability $e^{-(\Delta E/kT)}$. A Monte Carlo step is defined as the completion of a sequence in which all molecules are moved once. The maximum displacement, Δ, of a molecule is fixed in order to obtain an acceptance ratio of approximately 50%.

The constant pressure simulations were run in a similar manner except that at the end of one MC step, a change in the volume of the simulation box was attempted. The volume change was accepted if $\Delta H \leqslant 0$, while if $\Delta H > 0$ the move was accepted with probability $e^{-(\Delta H/kT)}$ where ΔH is the enthalpy change, $\Delta H = \Delta E - P\Delta V$.

During the simulations, a molecular transfer control constraint was imposed so as to avoid phase separation. This was done by dividing the system into equal regions and restricting the fluctuations of the number of molecules in each region to maintain homogeneous density throughout the measurement volume. This technique, similar to that of Hoover and Ree [23] and Hansen and Verlet [13], has been shown by Adachi [24] to work for a small number of molecules. The number of regions was selected empirically as eight. With $N = 96$, this gives an average box population $v = 12$. The maximum allowable deviation, $\delta n \geqslant \Delta n$, where Δn is determined by

$$\Delta n^2 = \frac{2n}{\beta} \frac{\partial P}{\partial \varrho^*}\bigg|_T \tag{17}$$

The partial derivative is taken at constant temperature of the saturated liquid and was approximated as the slope of a trial P vs. ϱ^* curve taken near $\varrho^* = 0.13$. using this result, we chose $\delta n = 4$ for all temperatures except $T = 2$, where δn was taken to be 3. This constraint was found to be imposed never more than 5% of the total attempted moves and never below $\varrho^* = 0.09$.

Equilibrium was established by starting from a very low density and squeezing the length of the box until the desired density was reached. The resulting configuration was then run at a high temperature and cooled to the temperature of interest. This state was then used to collect data for the (T, ϱ^*) state point. Data for the pressure integration were collected through the density range 0.01 to 0.23 at every 0.01. Each point was run long enough so that equilibrium was assured by monitoring changes in the energy and pressure.

A test was made of the effect of different starting configurations on the equilibration and eventual outcome of the simulations. Various starting configurations were tried, ranging from the center of mass at lattice positions to random placement. The deviations in determination of the pressure had a maximum variance of 3%. These deviations yielded a change of less than 3% in the determination of chemical potential either by pressure integration of particle insertion.

Finite size effects were investigated by simulations of a system of 256 hexamer molecules at $T = 10.0$ and $\varrho = 0.05$, 0.10 and 0.15 and comparing the results to the same state point with 96 molecules. The pressure and chemical potential data obtained from the two systems agreed within the 3% variance determined for the 96 molecule system.

The integration of A^r in Equation (1b) was done by fitting the integrand to a 6th order polynominal and integrating analytically. The ghost particle insertion was attempted at selected densities, shown in Table 1. At every 25 Monte Carlo steps, 100 insertions of the extra molecule, identical to those in the system, were attempted. This was done by randomly choosing the center of mass. In addition, for each insertion, 100 random orientation of the molecule were attempted to determine the energy, u, in Eq. (9). From Eq. (6), we see that only insertions which result in negative or small positive energies are useful in determining the μ^r. As density increases, the probability that a ghost particle will be inserted near or on top of another particle is increased significantly and very long runs are necessary at higher densities to generate reliable data. At a molecule density, $\varrho^* > 0.16$, the amount of CPU time to generate data for the ghost particle insertion became excessive. This effectively sets the upper density limit for which we could use this technique.

For higher densities one needs to apply Kirkwood's integration technique to obtain the chemical potentials. This method performs an insertion with $\zeta = \zeta_i$, where ζ_i is the largest molecule that can be inserted with good statistics. ζ_i was empirically determined by first obtaining an equilibrated state using constant pressure simulations. Once this equilibrated state was found, insertions were tried with various charging parameters. For most systems we chose $\zeta_i = 0.4$. Once the equilibrated state and ζ_i was established, the modified Widom method was used to determine $\mu^r_{\zeta_i}$. Then, starting from the previous equilibrated state, a separate series of constant pressure simulations was done to determine the average ensemble energies at various values of ζ. A thermodynamic integration over energy was then used for the integral in Equation (12), where the integral is evaluated numerically using a simple trapezoidal rule method. The average number of insertions accepted per simulation was $\sim 1.5 \times 10^5$. However, more insertions were needed at the highest density.

References

[1] S. Romano and K. Singer, "Calculation of the entropy of liquid chlorine and bromine by computer simulation", *Mol. Phys.*, **37,** 1765 (1979).

[2] B. Guillot and Y. Guissani, "Investigation of the chemical potential by molecular dynamics simulation" *Mol. Phys.*, **54,** 455 (1985).

[3] M. Wojcik, K.E. Gubbins and J.G. Powles, "Thermodynamics of symmetric two centre Lennard-Jones Liquids", *Mol. Phys.*, **45,** 1209 (1982).

[4] D. Fincham, N. Quirke and D.J. Tildesley, "Computer simulation of molecular liquid mixtures. I. A diatomic Lennard-Jones model for CO_2/C_2H_6", *J. Chem. Phys.*, **84,** 4535 (1986).

[5] N. Quirke, "The Calculation of Free Energies Using Computer Simulation", Proc. N.A.T.O. Summer School on Supersonic Conductors, Odense, Denmark 1980.

[6] U. Heinbuch and J. Fischer, "On the application of Widom's test particle method to homogeneous and inhomogeneous fluids", *Mol. Sim.*, **1,** 109 (1987).

[7] J.G. Powles, W.A.B. Evans and N. Quirke, "Non-destructive molecular-dynamics simulation of the chemical potential of a fluid", *Mol. Phys.*, **46,** 1347 (1982).

[8] K.S. Shing, and K.E. Gubbins, "The Chemical potential in dense fluids and fluid mixtures via computer simulation", *Mol. Phys.*, **46,** 1109 (1982).

[9] D.J. Adams, "Chemical potential of hard-sphere fluids by Monte Carlo methods", *Mol. Phys.*, **28,** 1241 (1974).

[10] J.M. Haile, "On the use of computer simulation to determine the excess free energy in fluid mixtures", *Fluid Phase Equilibria*, **26,** 103 (1986).

[11] M. Wojcik, and K.E. Gubbins, "Thermodynamics of hard dumbbell mixtures", *Mol. Phys.*, **49,** 1401 (1983).

[12] I. Aviram, and D.J. Tildesley, "A Monte Carlo study of mixtures of hard diatomic molecules", *Mol. Phys.*, **35,** 365 (1978).

[13] J.P. Hansen and L. Verlet, "Phase transitions of the Lennard-Jones system" *Phys. Rev.*, **184,** 151 (1969).
[14] B. Widom "Some topics in the theory of fluids", *J. Chem. Phy.*, **39,** 2808 (1963).
[15] C.H. Bennett, "Efficient estimation of the free energy differences from Monte Carlo data", *J. Comp. Phy.*, **22,** 245 (1976).
[16] M.J. De Oliviera, 1979, private communication to K.E. Gubbins, See [3] ref. 7.
[17] J.G. Kirkwood, "Statistical mechanics of liquid solutions", *Chem. Rev.*, **19,** 275 (1936).
[18] Shing, K.S. and S.T. Chung, "Computer Simulation Methods for the Calculation of Solubility in Supercritical Extraction Systems", Paper given at AIChE Annual Meeting, Chicago 1985.
[19] a) G. Jacucci and N. Quirke, "Monte Carlo calculation of the free energy difference between hard and soft core diatomic liquids", *Mol. Phys.*, **40,** 1005 (1980).
b) N. Quirke and G. Jacucci, "Energy difference functions in Monte Carlo simulations: Application to (1) the calculation of the free energy of liquid nitrogen, (2) the fluctuation of Monte Carlo averages", *Mol. Phys.*, **45,** 823 (1982).
[20] I. Nezbeda, "Virial expansion and an improved equation of state for the hard convex molecule system", *Chem. Phys Lett.*, **41,** 55 (1976).
[21] N. Metropolis, A.W. Rosenbluth, M.N. Rosenbluth, A.H. Teller and E. Teller, "Equation of state calculations by fast computing machines", *J. Chem. Phys.*, **21,** 1087 (1953).
[22] M. Rao, C. Pangali and B.J. Berne, "On the force bias Monte Carlo simulation of water: methodology, optimization and comparison with molecular dynamics", *Mol. Phys.*, **37,** 1773 (1979).
[23] W.G. Hoover and F.H. Ree, "Use of computer experiments to locate the melting transistion and calculate the entropy in the solid phase", *J. Chem. Phys.*, **47,** 4873 (1967).
[24] Y. Adachi, and H. Sugle, "Monte Carlo simulation of the P-V-T behavior of argon in metastable and unstable regions" *I. Ch. E.*, **21,** 604 (1981).